Performance of the CALET calorimeter for GeV energy gamma-ray observations

Nicholas Cannady (Louisiana State University)
for the CALET Collaboration

Submitted to ApJS

See also: **E1.17-0022-18** (Mori & Asaoka): GeV-energy transients with CALET

The CALET Team

O. Adriani[25], Y. Akaike[2], K. Asano[7], Y. Asaoka[9,31], M.G. Bagliesi[29], E. Berti[25], G. Bigongiari[29], W.R. Binns[32], S. Bonechi[29], M. Bongi[25], P. Brogi[29], A. Bruno[15], J.H. Buckley[32], N. Cannady[13], G. Castellini[25], C. Checchia[26],M.L. Cherry[13], G. Collazuol[26], V. Di Felice[28], K. Ebisawa[8], H. Fuke[8], T.G. Guzik[13], T. Hams[3], N. Hasebe[31], K. Hibino[10], M. Ichimura[4], K. Ioka[34], W. Ishizaki[7], M.H. Israel[32], K. Kasahara[31], J. Kataoka[31], R. Kataoka[17], Y. Katayose[33], C. Kato[23], Y.Kawakubo[1], N. Kawanaka[30], K. Kohri [12], H.S. Krawczynski[32], J.F. Krizmanic[2], T. Lomtadze[27], P. Maestro[29], P.S. Marrocchesi[29], A.M. Messineo[27], J.W. Mitchell[15], S. Miyake[5], A.A. Moiseev[3], K. Mori[9,31], M. Mori[20], N. Mori[25], H.M. Motz[31], K. Munakata[23], H. Murakami[31], S. Nakahira[9], J. Nishimura[8], G.A De Nolfo[15], S. Okuno[10], J.F. Ormes[25], S. Ozawa[31], L. Pacini[25], F. Palma[28], V. Pal'shin[1], P. Papini[25], A.V. Penacchioni[29], B.F. Rauch[32], S.B. Ricciarini[25], K. Sakai[3], T. Sakamoto[1], M. Sasaki[3], Y. Shimizu[10], A. Shiomi[18], R. Sparvoli[28], P. Spillantini[25], F. Stolzi[29], S. Sugita[1], J.E. Suh[29], A. Sulaj[29], I. Takahashi[11], M. Takayanagi[8], M. Takita[7], T. Tamura[10], N. Tateyama[10], T. Terasawa[7], H. Tomida[8], S. Torii[9,31], Y. Tunesada[19], Y. Uchihori[16], S. Ueno[8], E. Vannuccini[25], J.P. Wefel[13], K. Yamaoka[14], S. Yanagita[6], A. Yoshida[1], and K. Yoshida[22]

1) Aoyama Gakuin University, Japan
2) CRESST/NASA/GSFC and Universities Space Research Association, USA
3) CRESST/NASA/GSFC and University of Maryland, USA
4) Hirosaki University, Japan
5) Ibaraki National College of Technology, Japan
6) Ibaraki University, Japan
7) ICRR, University of Tokyo, Japan
8) ISAS/JAXA Japan
9) JAXA, Japan
10) Kanagawa University, Japan
11) Kavli IPMU, University of Tokyo, Japan
12) KEK, Japan
13) Louisiana State University, USA
14) Nagoya University, Japan
15) NASA/GSFC, USA
16) National Inst. of Radiological Sciences, Japan
17) National Institute of Polar Research, Japan
18) Nihon University, Japan
19) Osaka City University, Japan
20) Ritsumeikan University, Japan
21) Saitama University, Japan
22) Shibaura Institute of Technology, Japan
23) Shinshu University, Japan
24) University of Denver, USA
25) University of Florence, IFAC (CNR) and INFN, Italy
26) University of Padova and INFN, Italy
27) University of Pisa and INFN, Italy
28) University of Rome Tor Vergata and INFN, Italy
29) University of Siena and INFN, Italy
30) University of Tokyo, Japan
31) Waseda University, Japan
32) Washington University-St. Louis, USA
33) Yokohama National University, Japan
34) Yukawa Institute for Theoretical Physics, Kyoto University, Japan

The CALorimetric Electron Telescope

- Deployed on the ISS since 2015/08
  - **Advanced Stellar Compass (ASC)**
  - CALET Gamma-ray Burst Monitor (CGBM)
    - Hard X-ray Monitor (HXM)
    - Soft Gamma-ray Monitor (SGM)
  - Calorimeter (CAL)

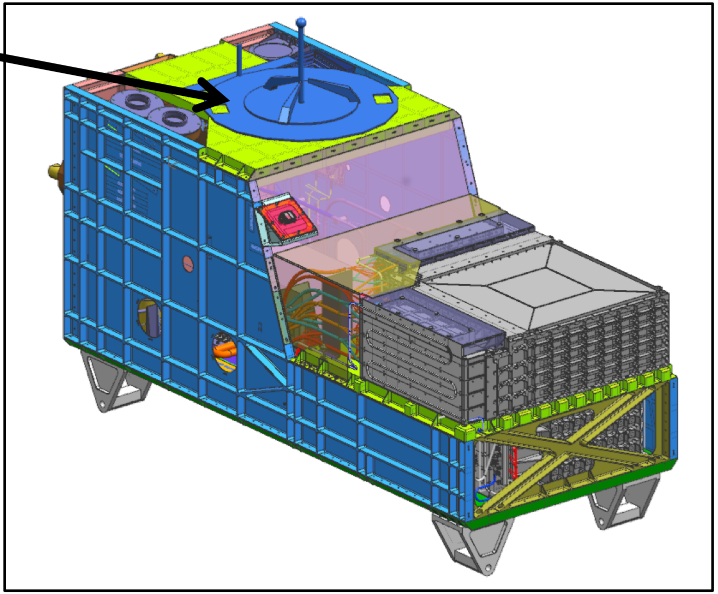

The CALorimetric Electron Telescope

- Deployed on the ISS since 2015/08
  - Advanced Stellar Compass (ASC)
  - **CALET Gamma-ray Burst Monitor (CGBM)**
    - **Hard X-ray Monitor (HXM)**
    - **Soft Gamma-ray Monitor (SGM)**
  - Calorimeter (CAL)

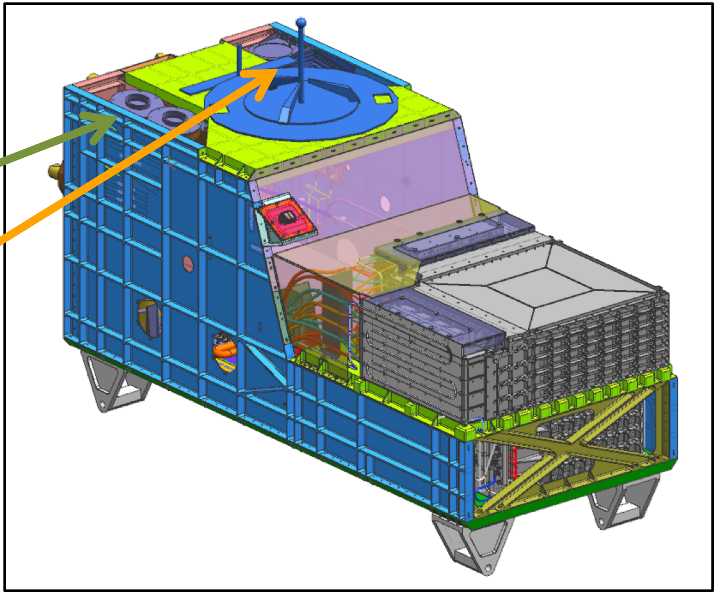

The CALorimetric Electron Telescope

- Deployed on the ISS since 2015/08
  - Advanced Stellar Compass (ASC)
  - CALET Gamma-ray Burst Monitor (CGBM)
    - Hard X-ray Monitor (HXM)
    - Soft Gamma-ray Monitor (SGM)
  - **Calorimeter (CAL)**

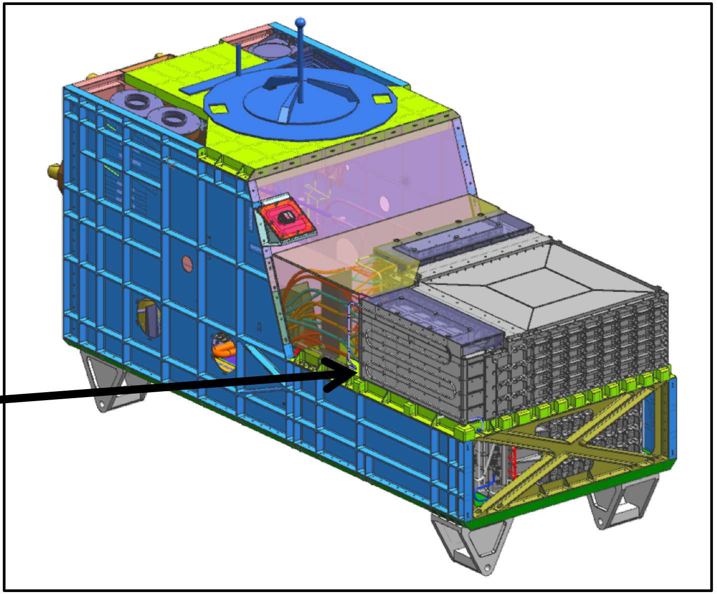

CALET-CAL

- Observation targets
  - Electrons (10 GeV – 20 TeV)
  - Gamma-rays (1 GeV – 1 TeV)
  - Protons and nuclei (to ~1 PeV)

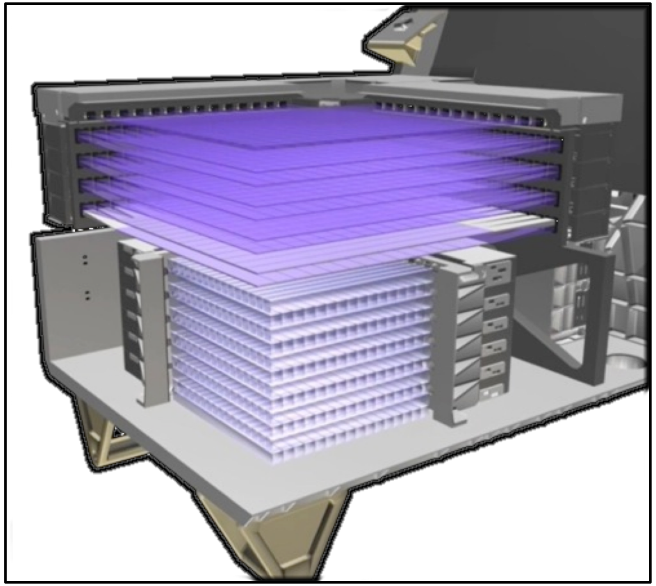

CALET-CAL

- CAL subsystems
  - Charge Detector (CHD)
    - Plastic scintillating paddles (32mm x 10mm x 450mm)
  - Imaging Calorimeter (IMC)
    - Fine plastic scintillating fibers (1mm x 1mm x 448mm)
    - Inactive tungsten sheets
    - Total 3 radiation lengths
  - Total Absorption Calorimeter (TASC)
    - Lead tungstate logs (19mm x 20mm x 326mm)
    - Total 27 radiation lengths

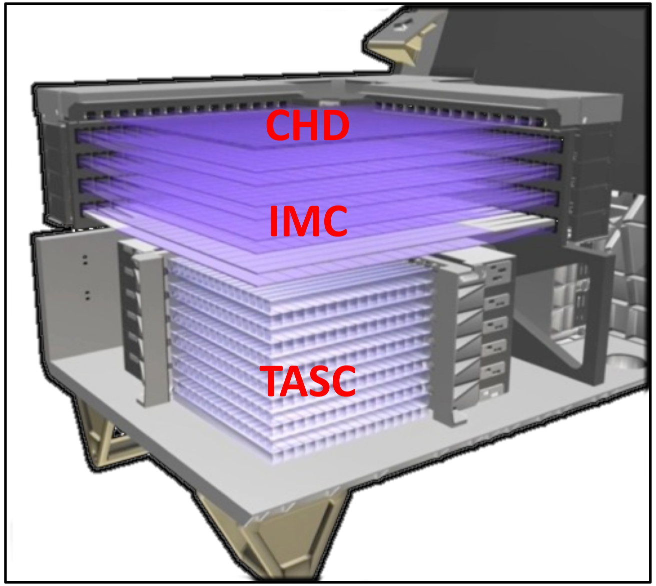

Showers in the CAL

Gamma-ray candidate
Edep sum ~400 GeV

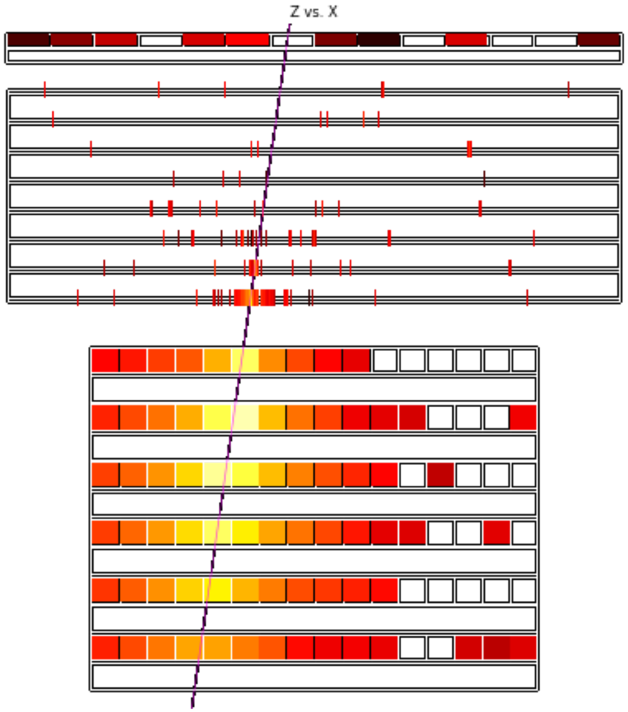

Helium candidate
Edep sum ~400 GeV

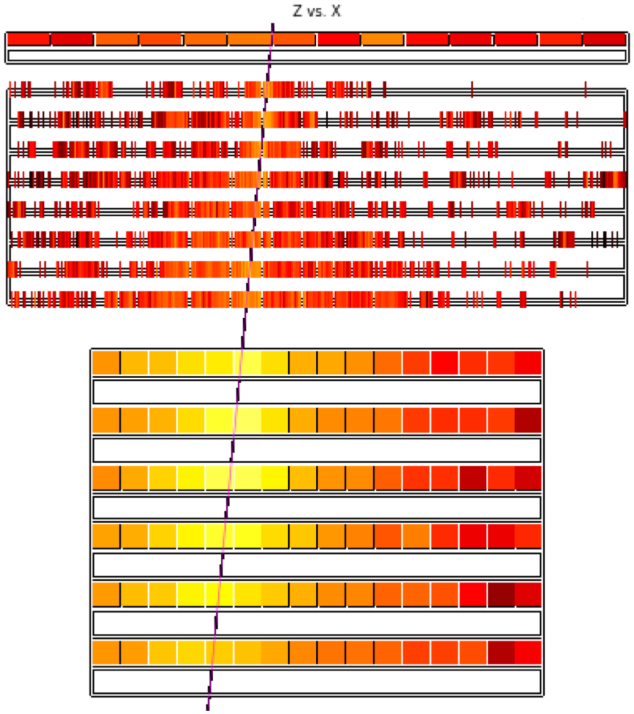

Gamma-ray event selection

- Preselection
  - Offline trigger
  - Geometry
  - Tracking
- Shower shape
  - IMC concentration
  - Albedo
  - **K-cut (90% eff.)**
- Charge zero
  - CHD hit filter
  - CHD max filter
  - IMC1 hit filter

Gamma-ray event selection

- Preselection
  - Offline trigger
  - **Geometry**
  - Tracking
- Shower shape
  - IMC concentration
  - Albedo
  - K-cut (90% eff.)
- Charge zero
  - CHD hit filter
  - CHD max filter
  - IMC1 hit filter

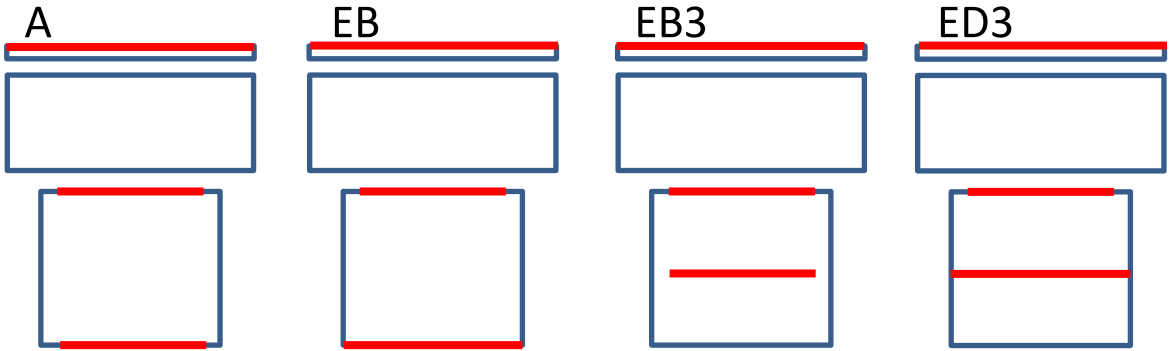

Acceptance	Conditions			Geom. Fact. [$cm^2 sr$]
A	CHD top	TASC top*	TASC 6y bottom*	419.1
EB	CHD top	TASC top*	TASC 6y bottom	91.03
ED	CHD top	TASC top*	TASC path > 24 cm	121.6
EB3	CHD top	TASC top*	TASC 3y bottom*	51.97
ED3	CHD top	TASC top*	TASC 3y bottom	127.9
E	CHD top	TASC top*		373.8

Table 3.1: Requirements for the LE-γ geometrical conditions. The conditions marked with asterisks denote that the intersection point must be more than 2 cm from the edge of the layer boundary.

Gamma-ray event selection

- Preselection
  - Offline trigger
  - Geometry
  - **Tracking**
- Shower shape
  - IMC concentration
  - Albedo
  - K-cut (90% eff.)
- Charge zero
  - CHD hit filter
  - CHD max filter
  - IMC1 hit filter

- EM Track
  - Developed for electromagnetic shower tracking
  - Used for the electron analysis
- CC Track
  - Developed specifically for low-energy gamma-rays
  - Increased sensitivity below 10 GeV

Requirements on track reconstruction

- $2 < N_{px} < 8$
- $2 < N_{py} < 8$
- $|N_{px} - N_{py}| \leq 1$
- Consistency with TASC 1x

N_p: number of IMC layers used in track reconstruction

Gamma-ray event selection

- Preselection
  - Offline trigger
  - Geometry
  - Tracking
- Shower shape
  - IMC concentration
  - Albedo
  - **K-cut (90% eff.)**
- Charge zero
  - CHD hit filter
  - CHD max filter
  - IMC1 hit filter

$$K = \log_{10} F_E + \frac{1}{2} R_E$$

F_E: fraction of TASC energy in bottom layer
R_E: lateral spread of TASC energy deposits

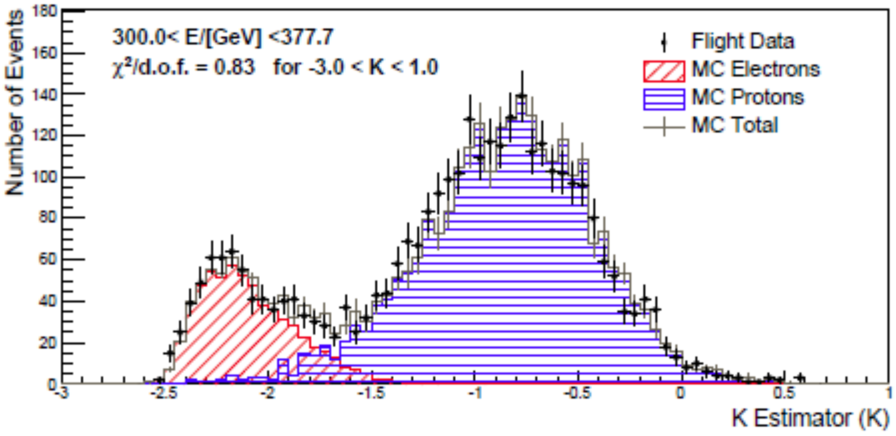

FIG. 2. An example of K-estimator distribution in the $300 < E < 378$ GeV bin. The reduced chi-square of the fit in the K-estimator range from -3 to 1 is 0.83.

O. Adriani et al., PRL 119, 181101 (2017) supplemental material

Gamma-ray event selection

- Preselection
  - Offline trigger
  - Geometry
  - Tracking
- Shower shape
  - IMC concentration
  - Albedo
  - K-cut (90% eff.)
- Charge zero
  - **CHD hit filter**
  - **CHD max filter**
  - **IMC1 hit filter**

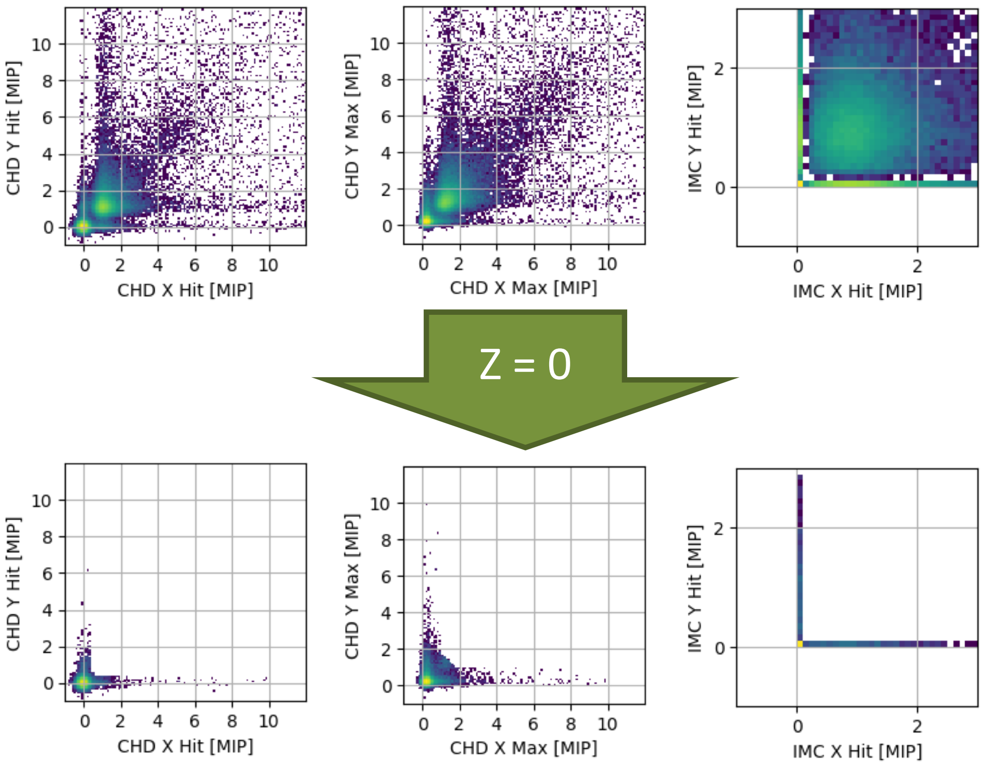

Gamma-ray event selection

- Preselection
  - Offline trigger
  - Geometry
  - Tracking
- Shower shape
  - IMC concentration
  - Albedo
  - K-cut (90% eff.)
- Charge zero
  - CHD hit filter
  - CHD max filter
  - IMC1 hit filter

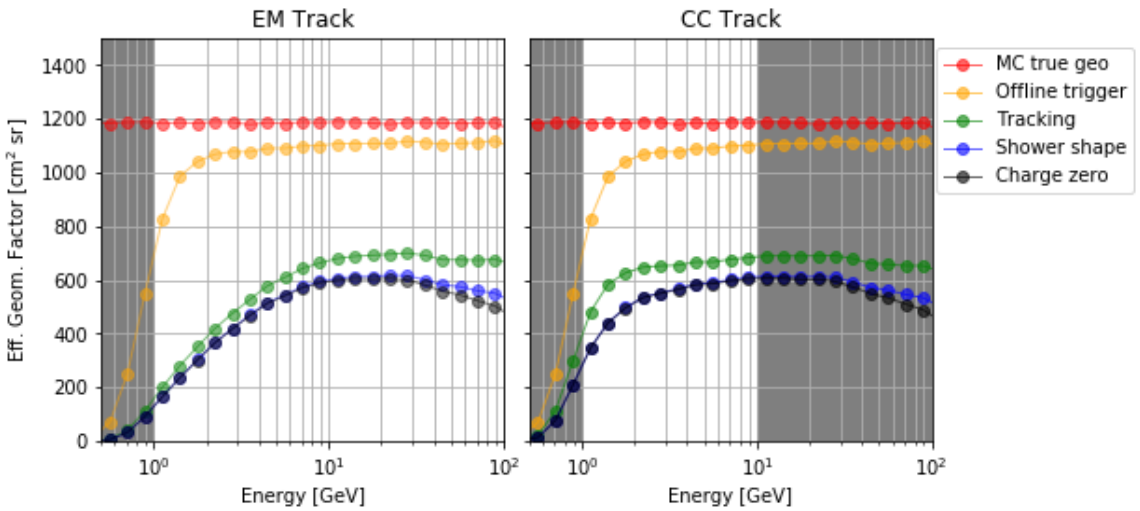

ISS structures

- Unexpected background source
  - ISS structures in CAL field of view
  - Secondary photons from cosmic ray interactions in material
  - Fixed structures – masked
  - Periodic structures (solar panels, radiators, etc.)
  - Non-periodic structures (SSRMS, ...)

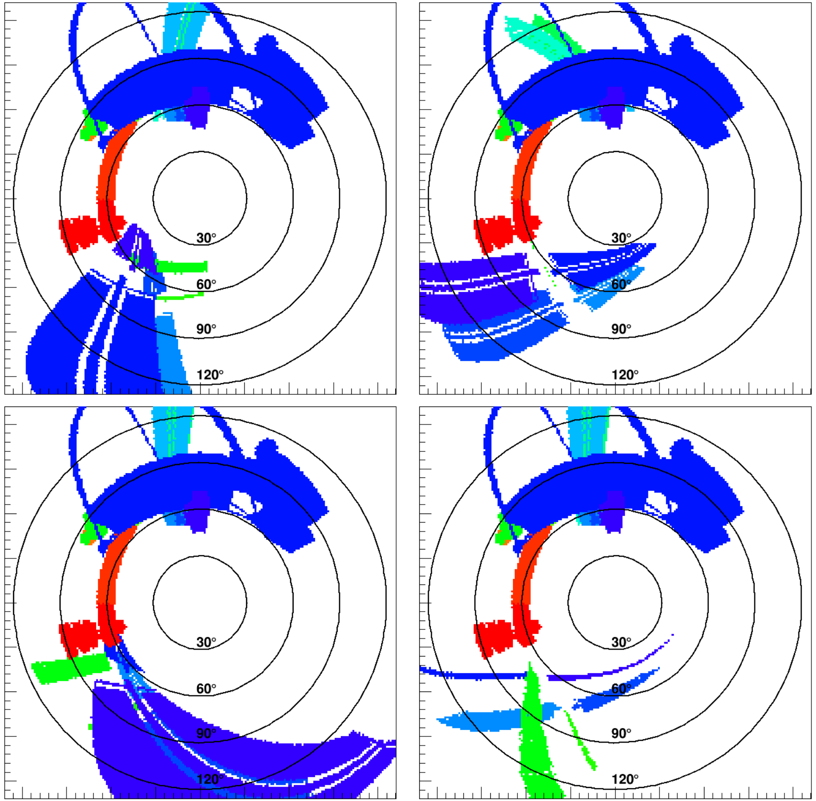

Dataset

- Simulated:

  http://cosmos.n.kanagawa-u.ac.jp/

  - EPICS/COSMOS package used for simulation
  - Thrown isotropic from sphere
  - 0.1 GeV – 1000 GeV, distributed ~ E^{-1}
  - 3.2×10^{7} events per decade of energy
- Flight
  - First two years of LE-γ run data (2015/11 – 2017/10)
  - Reduced threshold of ~1 GeV
  - Active at low geomagnetic latitudes

Effective area

EM Track reaches maximum (~400 cm^2) at E ~10 GeV

Events with E < 1 GeV not included in present analysis

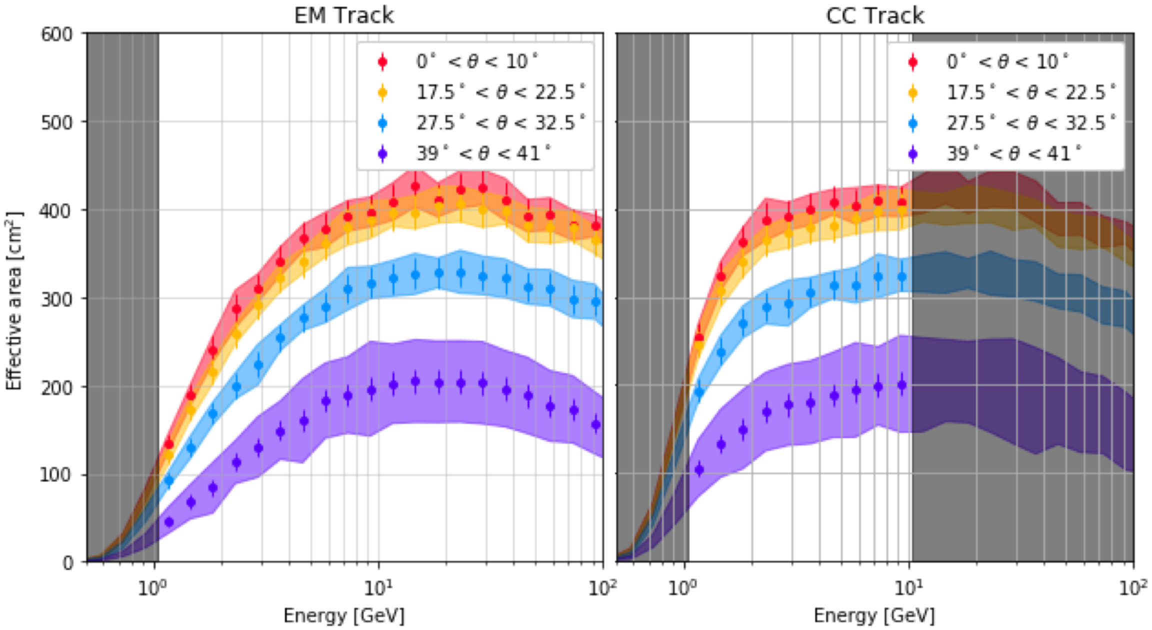

CC Track reaches maximum at E ~2 GeV

CC Track not used above 10 GeV

Effective area determined using EPICS simulations

Angular resolution

- 68% containment radius in angular error
- Fit by empirical scaling function

$$S_p(E, N_p) = \sqrt{c_0^2 + c_1^2 E^{-2\beta}(1 + E^{\alpha})}$$

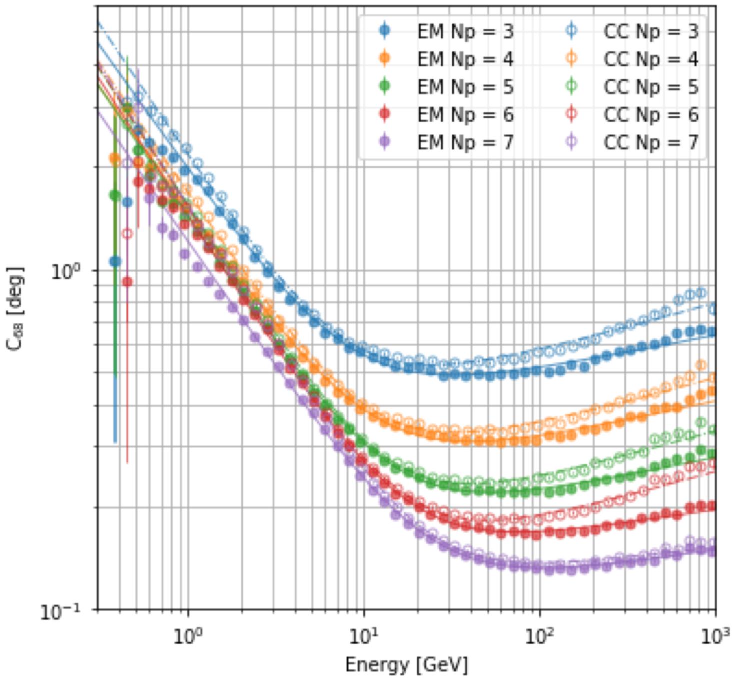

Angular resolution

- 68% containment radius in angular error
- Fit by empirical scaling function

$$S_p(E, N_p) = \sqrt{c_0^2 + c_1^2 E^{-2\beta}(1 + E^{\alpha})}$$

- Point-spread function constructed with scaled angular error
- Fit by pair of King functions,

$$K(x, \sigma, \gamma) = \frac{1}{2\pi\sigma^2}\left(1 - \frac{1}{\gamma}\right)\left[1 + \frac{1}{2\gamma} \cdot \frac{x^2}{\sigma^2}\right]^{-\gamma}$$

K (core)
K (tail)

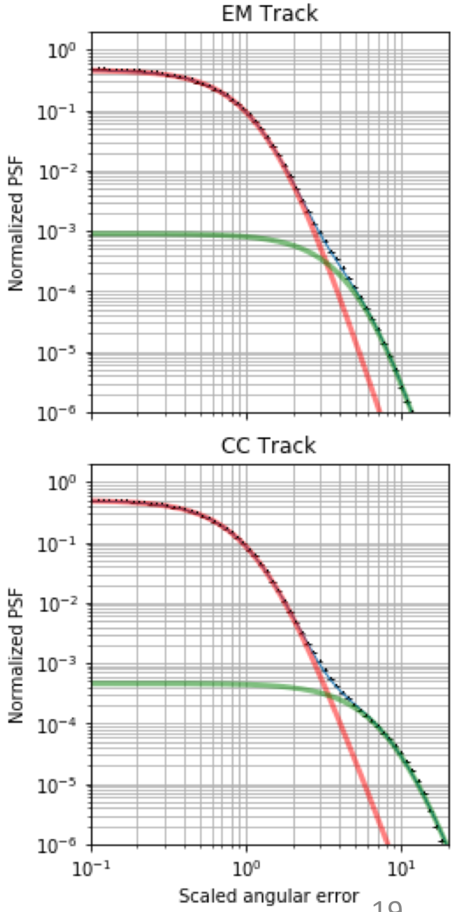

Flight data PSF

- Signals from Crab, Geminga, Vela used to validate simulated PSF
- Construct distribution of events in region in scaled angular error

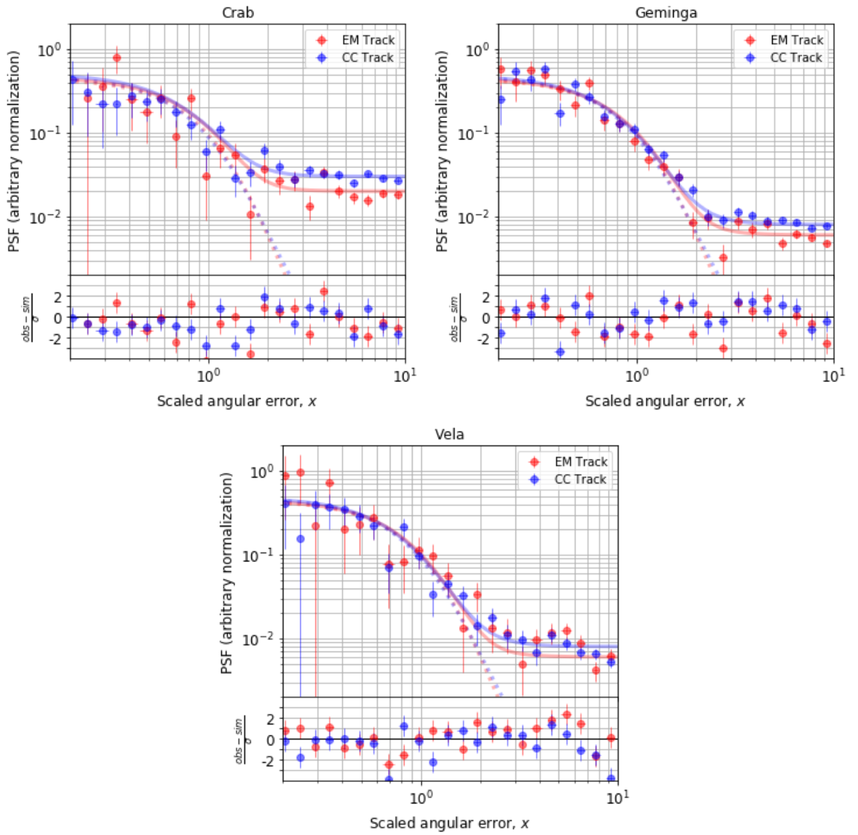

Flight data PSF

- Signals from Crab, Geminga, Vela used to validate simulated PSF
- Construct distribution of events in region in scaled angular error

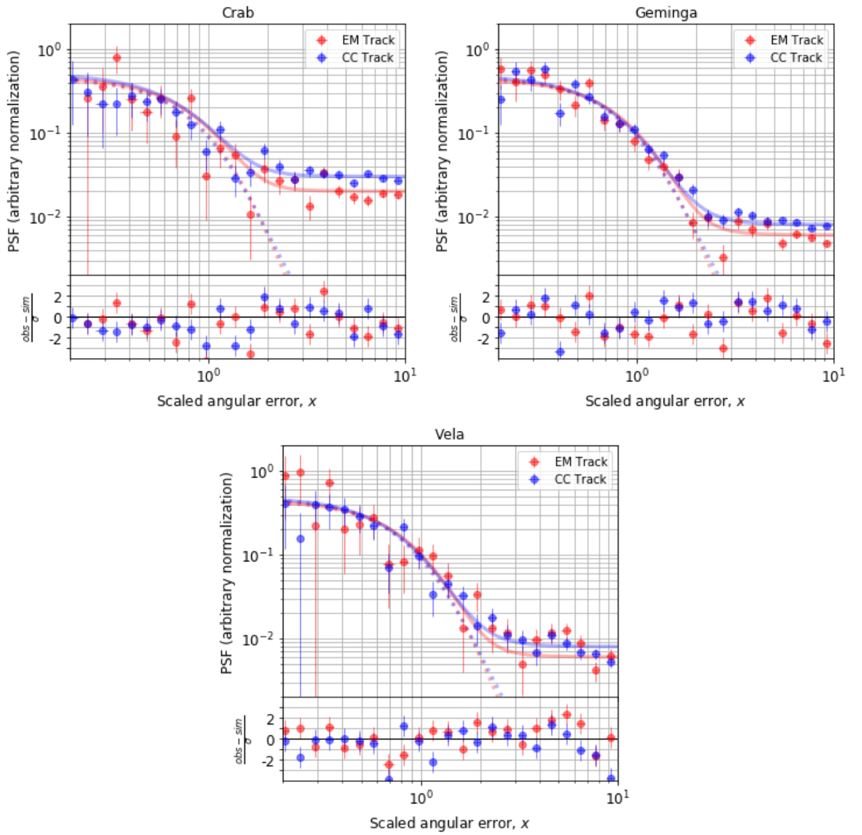

- Constant background term present
  - Galactic diffuse emission
  - Residual charged particles

Flux validation with pulsars

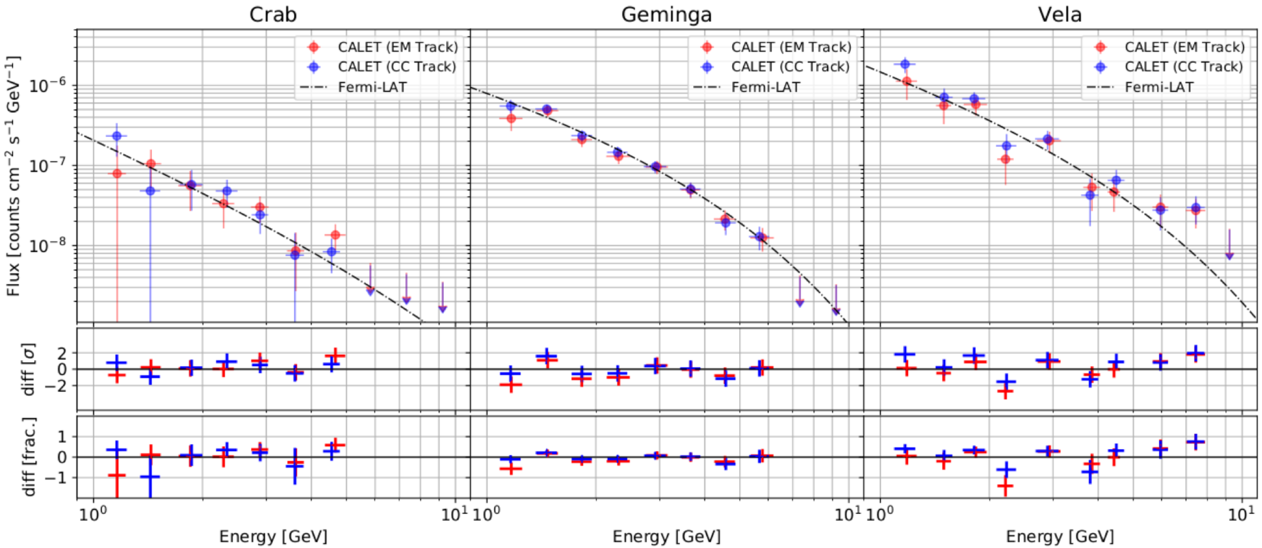

LAT fluxes:

Crab:
Abdo et al. 2009

Geminga:
Abdo et al. 2010

Vela:
Abdo et al. 2009

Agreement of fluxes with Fermi-LAT published parameterizations

Crab	χ^2 = 4.64 (EM), 4.16 (CC)	ndof = 7
Geminga	χ^2 = 6.73 (EM), 5.74 (CC)	ndof = 8
Vela	not consistent – systematic effects near edge of FOV	

Fermi-LAT diffuse comparison

- **Fermi-LAT PASS-08 data** for 08/04/2008 – 03/12/2017 taken from public archive
- CALET exposure applied to the derived flux map to determine expectation
- Comparison used to validate CALET diffuse observation

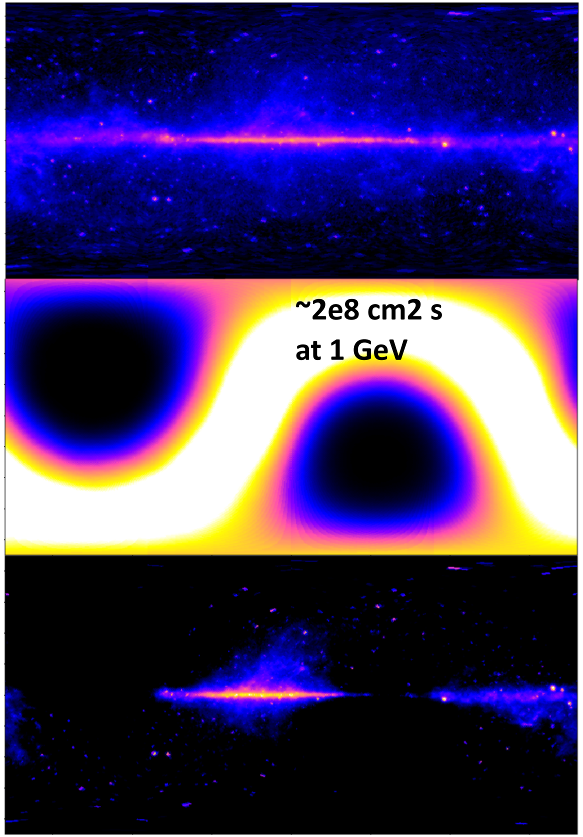

Fermi-LAT diffuse comparison

- Fermi-LAT PASS-08 data for 08/04/2008 – 03/12/2017 taken from public archive

- **CALET exposure** applied to the derived flux map to determine expectation

- Comparison used to validate CALET diffuse observation

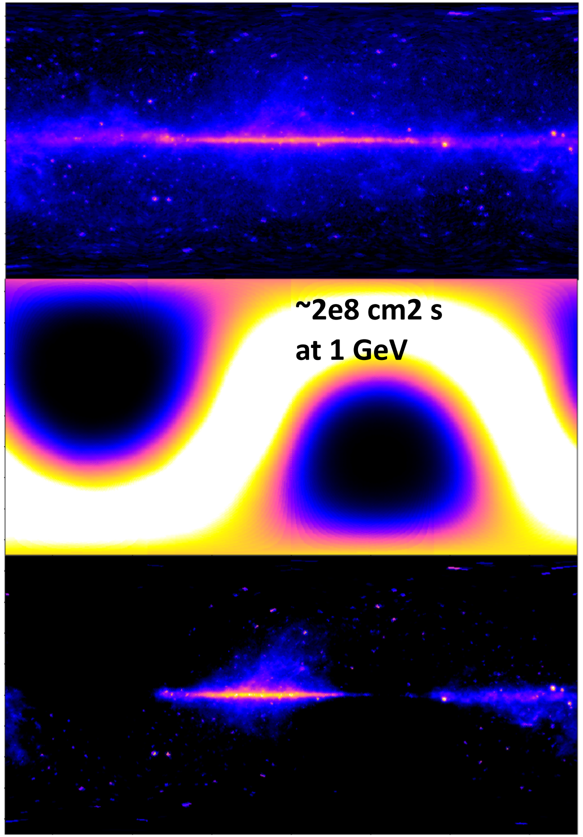

Fermi-LAT diffuse comparison

- Fermi-LAT PASS-08 data for 08/04/2008 – 03/12/2017 taken from public archive
- CALET exposure applied to the derived flux map to determine expectation
- Comparison used to validate CALET diffuse observation

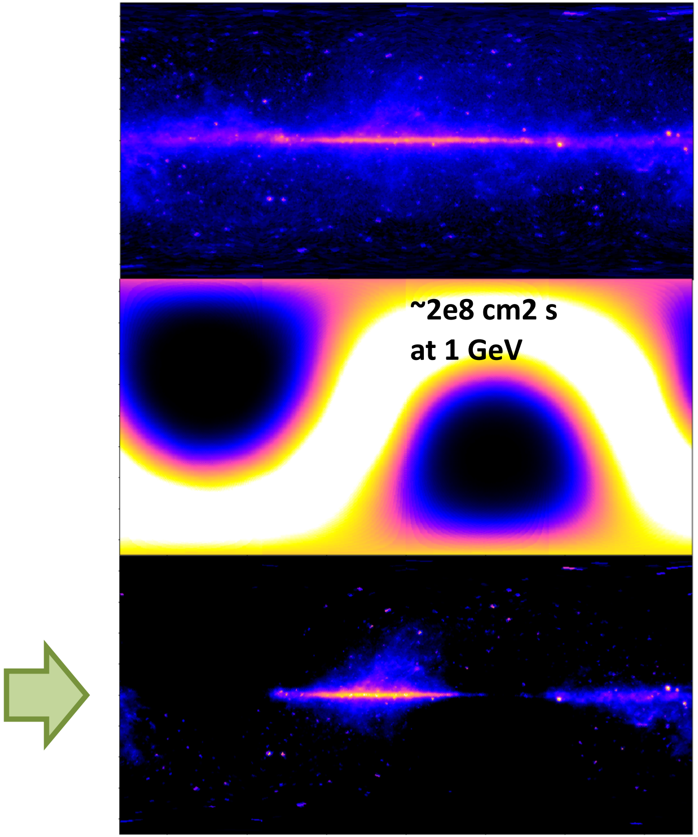

Restricted FOV

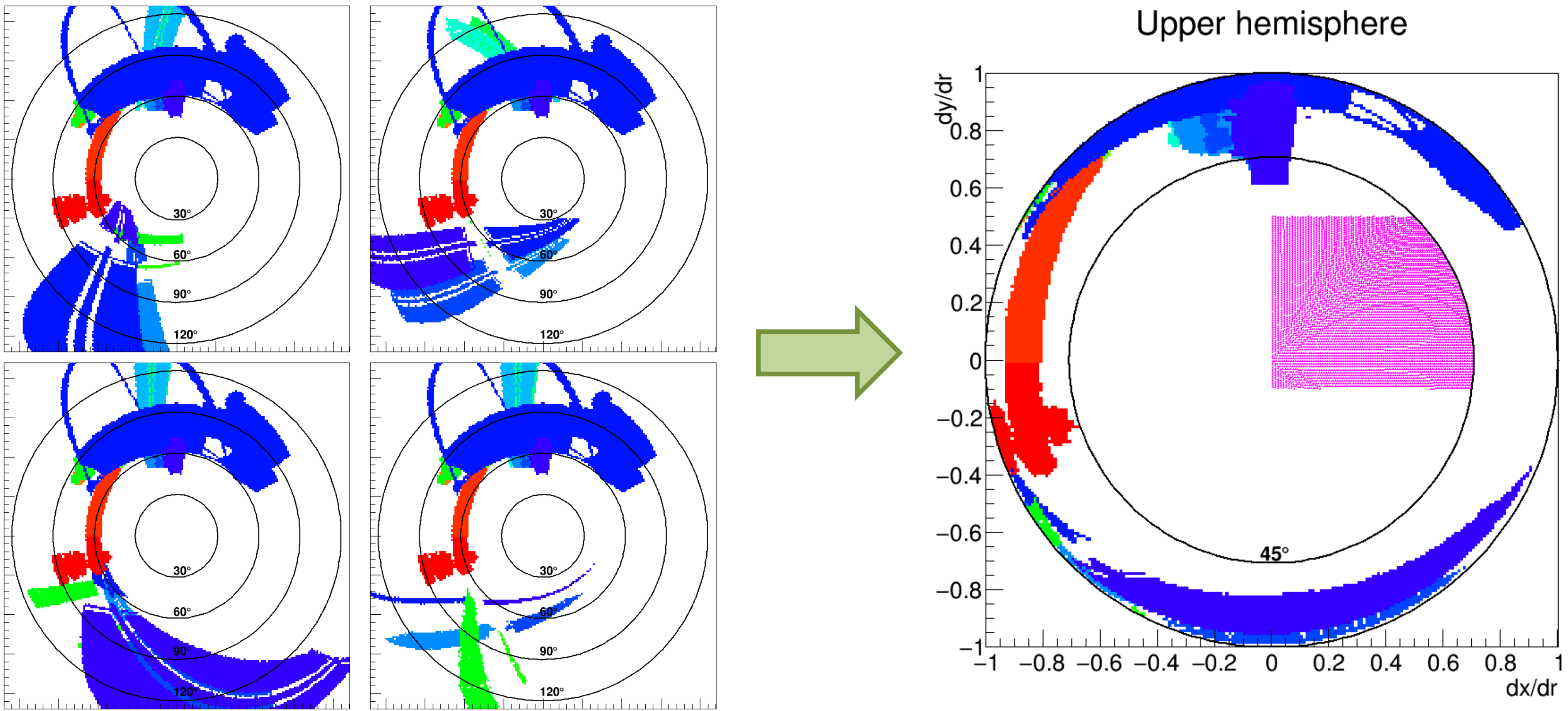

Galactic latitude projection

- Region: galactic latitude |l| < 80°
- Project events onto galactic latitude

- EM Track: consistent
- CC Track: excess at higher latitudes
  - Charged particles
  - Unaccounted-for ISS structure
  - Point sources

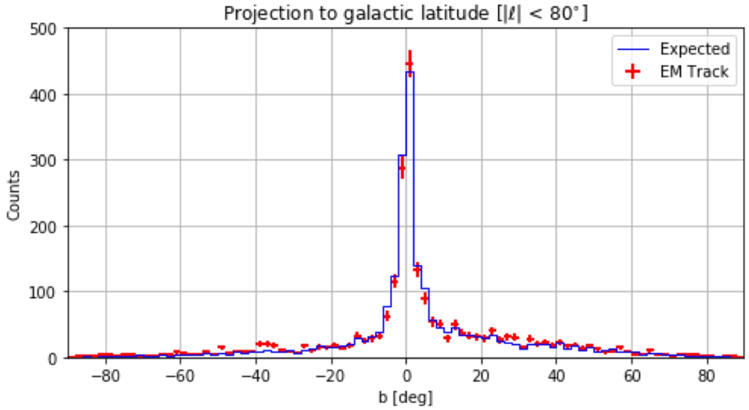

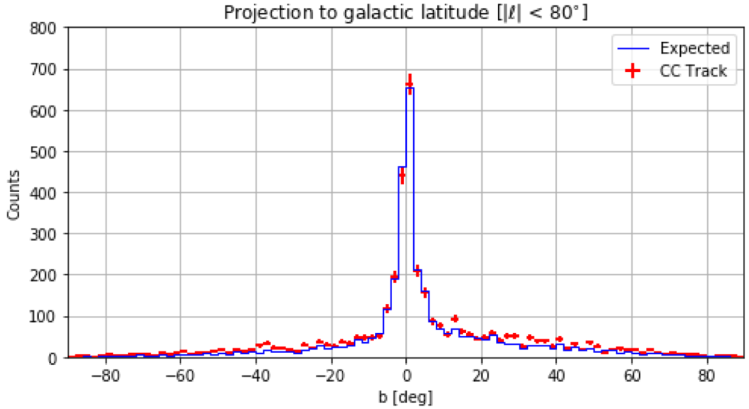

On- and off-plane regions

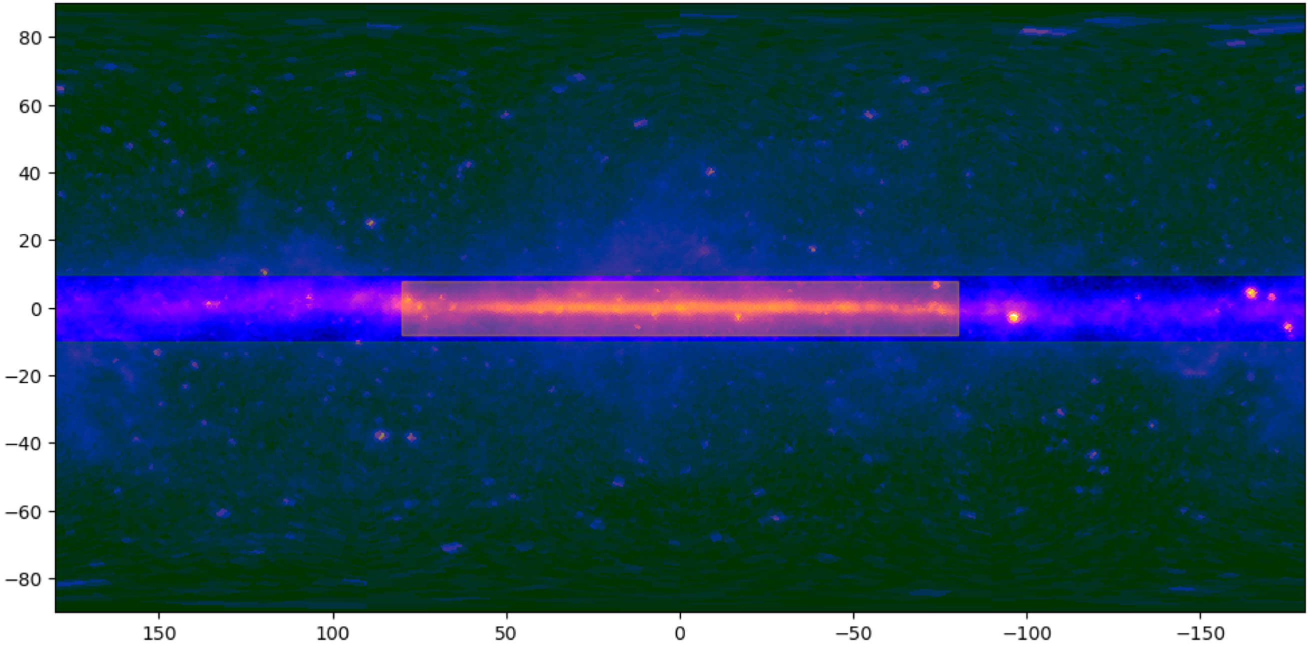

On-plane:

$|l| < 80°$

$|b| < 8°$

Off-plane:

$|b| > 10°$

Averaged fluxes

On-plane consistent:

EM: $\chi^2 = 16.5$ (19 dof)

CC: $\chi^2 = 5.31$ (10 dof)

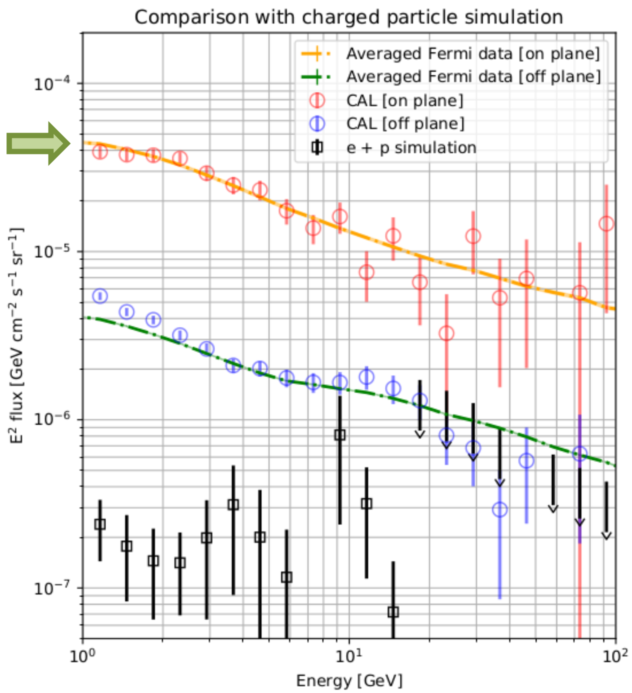

EM Track

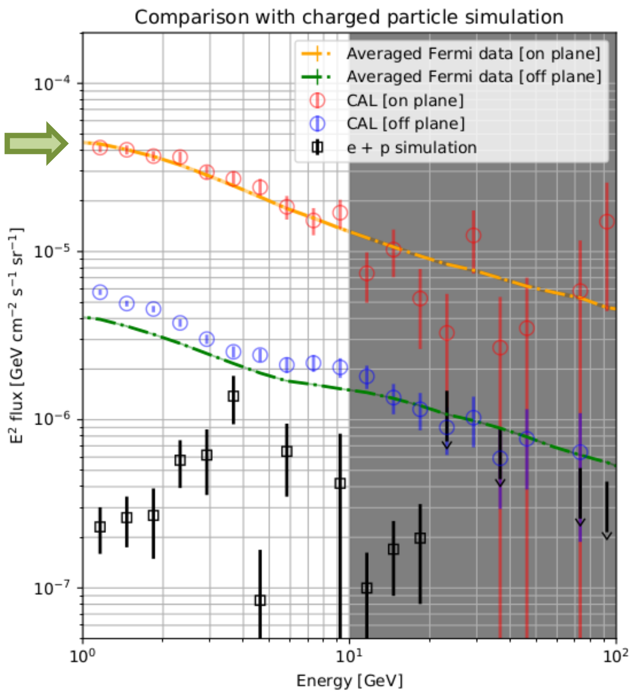

CC Track

Averaged fluxes

On-plane consistent:
EM: $\chi^2 = 16.5$ (19 dof)
CC: $\chi^2 = 5.31$ (10 dof)

Off-plane excess over expectation

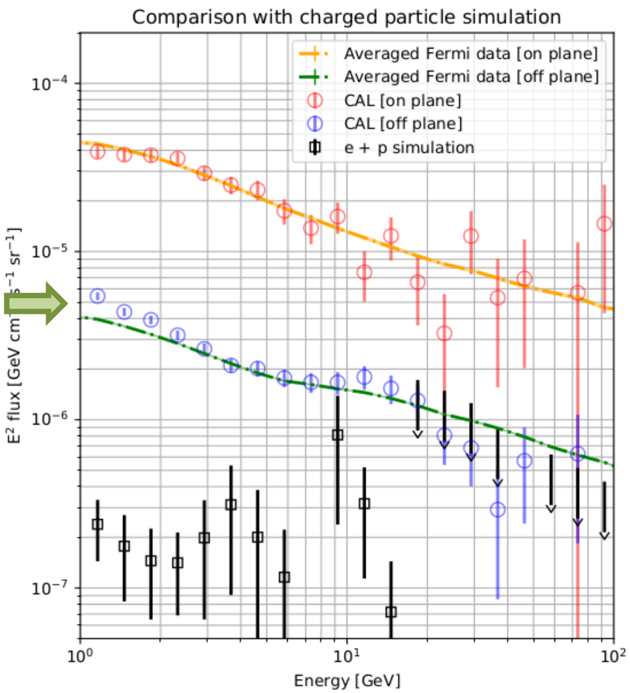

EM Track

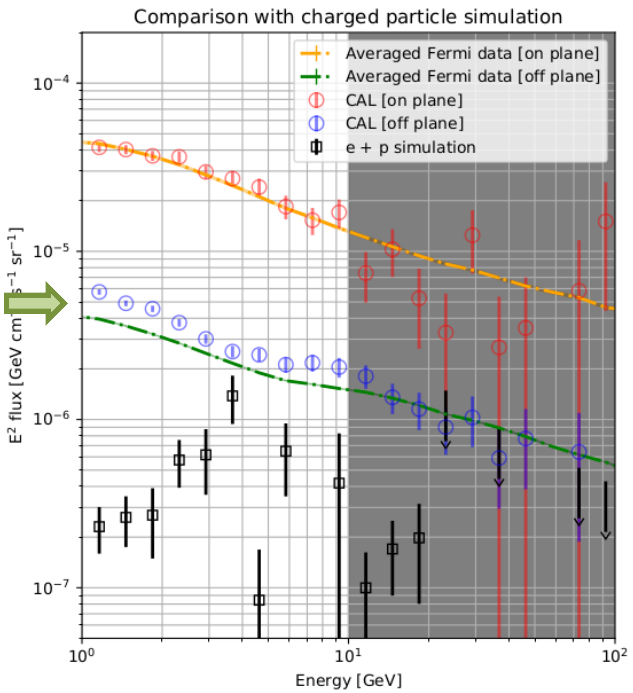

CC Track

Averaged fluxes

On-plane consistent:
EM: $\chi^2 = 16.5$ (19 dof)
CC: $\chi^2 = 5.31$ (10 dof)

Off-plane excess over expectation

Charged particle sim.
- Electrons (CALET flux)
- Protons
    - Low-energy: PAMELA
    - High-energy: AMS-02 and CREAM-III
- Can’t account for all low-energy excess

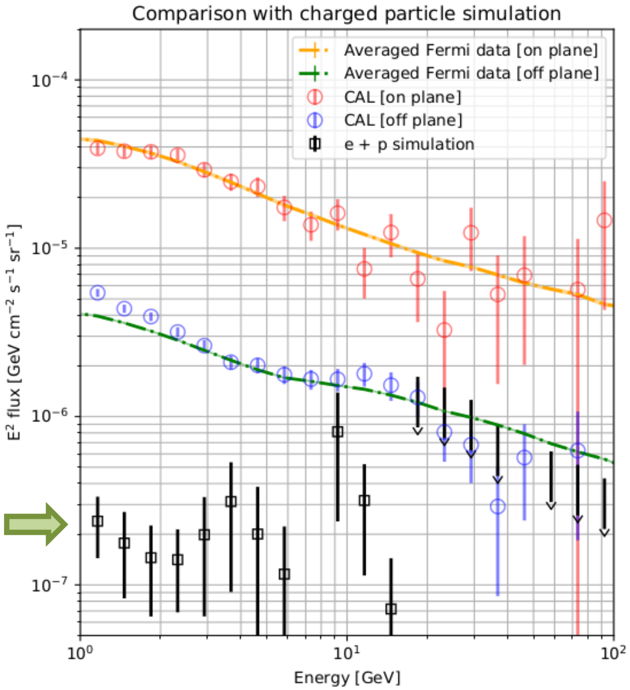

EM Track

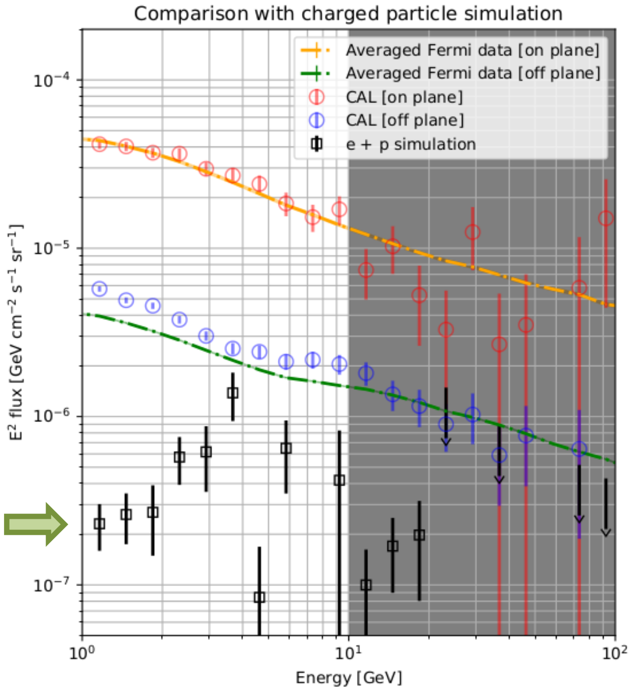

CC Track

Conclusions

- CALET observing gamma-rays E ≥ 1 GeV
- Instrument characterized using EPICS simulations
  - Effective area ~400 cm^2 above 2 GeV
  - Angular resolution < 2° above 1 GeV
    (< 0.2° above 10 GeV)
  - Energy resolution ~12% at 1 GeV
    ~5% at 10 GeV
- Simulated IRFs consistent with 2 years of flight data
- Consistency in signal-dominated regions with Fermi-LAT
- Residual background in low-signal regions
  (under investigation)

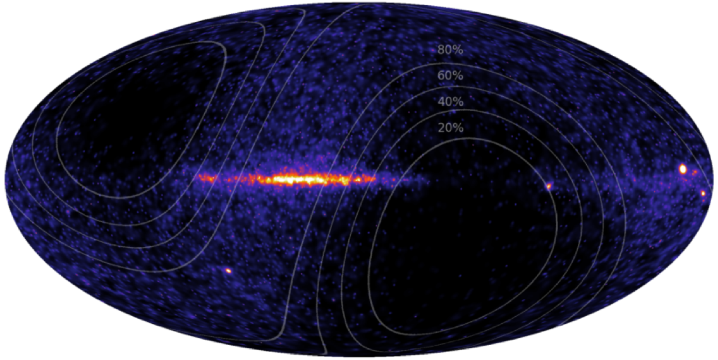

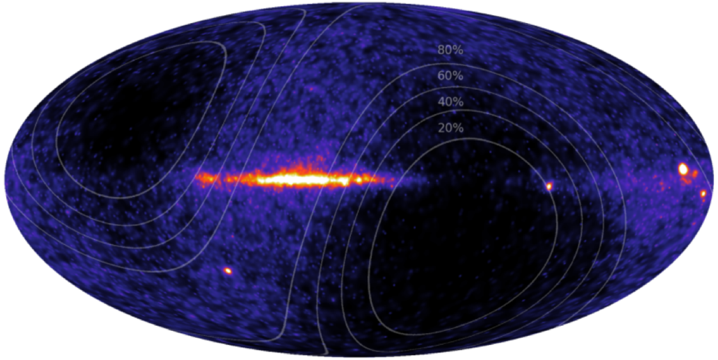

See also: **E1.17-0022-18** (Mori & Asaoka): GeV-energy transients with CALET

Backup

Energy reconstruction

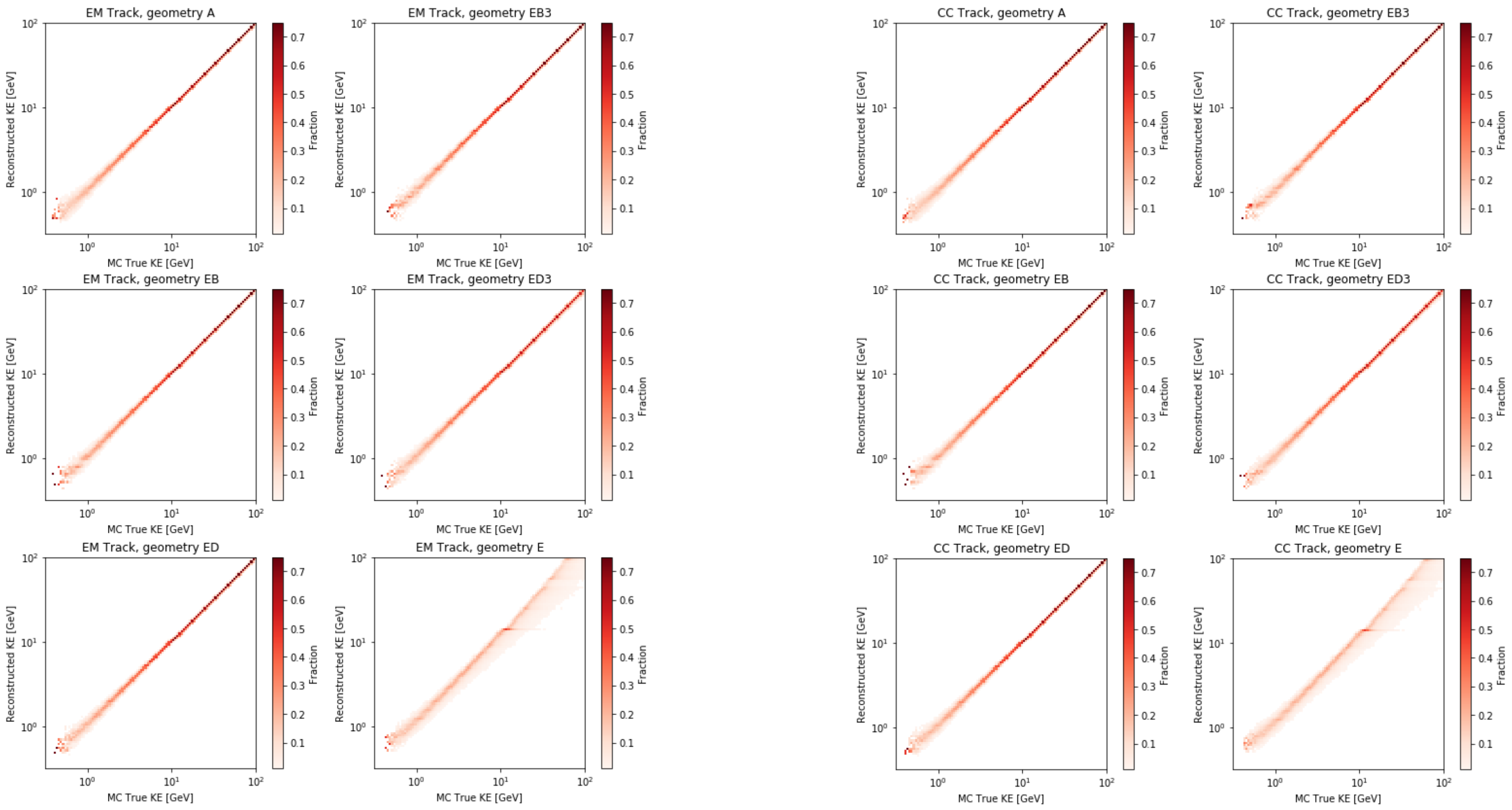

Absolute pointing accuracy

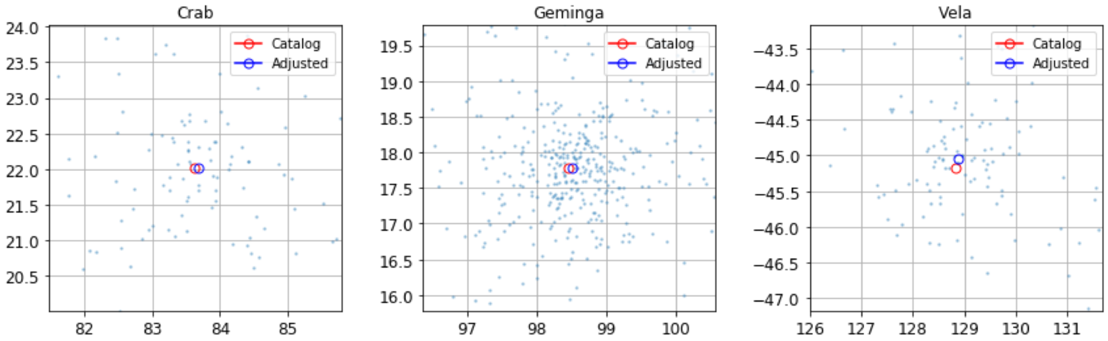

Source	Error, pre [deg]	Error, post [deg]
Crab	0.11	0.049
CTA 102	0.12	0.048
Geminga	0.047	0.018
Vela	0.19	0.088

Table 2. Error in the mean position of candidates associated with different point-sources before and after application of the correction quaternion.

- Overall rotation between catalog and CAL frames
  - Construct rotation quaternion to remove
  - Log-likelihood minimization using PSF for positions
- Residual errors after correction (< 0.1°)
  - Random in direction
  - Consistent with fitting errors
  - Statistics-limited pointing accuracy

Flux validation with pulsars

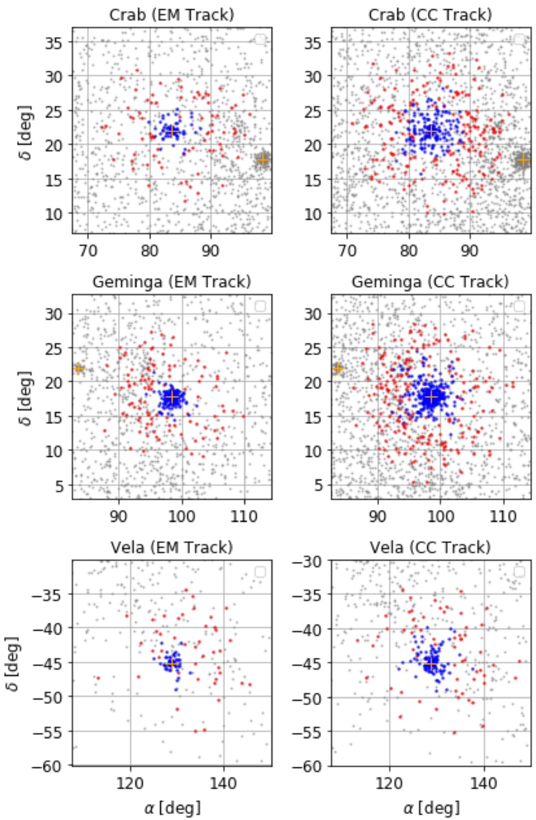

Associated with source (blue):

x < 2.6 (EM Track)

x < 3.4 (CC Track)

Background measurement (red):

4.5 < x < 6.5

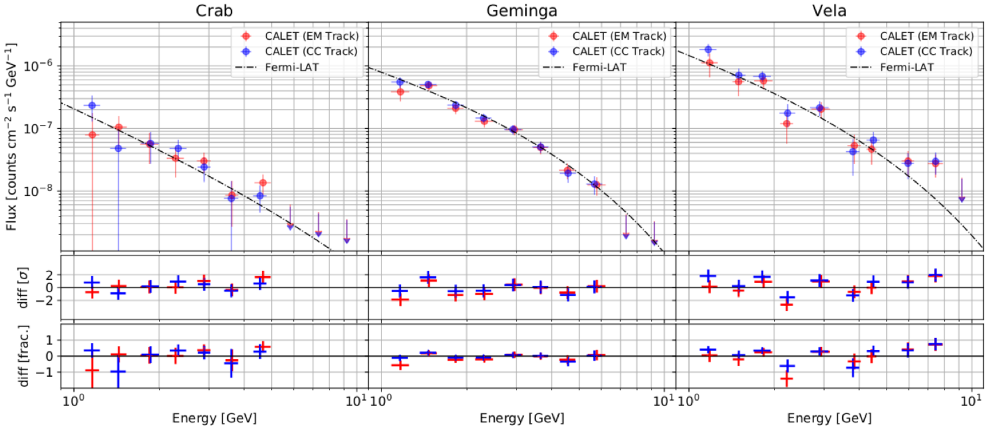

Geminga fit

High statistics and relatively low background fraction allow for fitting of the Geminga flux

Three models tried:

- Power law (PL)
- Broken power law (BPL)
- Cut-off power law (COPL)

- Simple PL not supported
- BPL and COPL both well fit
- COPL slightly favored over BPL
- Parameters within errors of Fermi-LAT published fit (Abdo et al. 2010)